

Where are my Neighbors? Exploiting Patches Relations in Self-Supervised Vision Transformer

Guglielmo Camporese
University of Padova, Italy

guglielmo.camporese@phd.unipd.it

Elena Izzo
University of Padova, Italy

elena.izzo@studenti.unipd.it

Lamberto Ballan
University of Padova, Italy

lamberto.ballan@unipd.it

Abstract

Vision Transformers (ViTs) enabled the use of transformer architecture on vision tasks showing impressive performances when trained on big datasets. However, on relatively small datasets, ViTs are less accurate given their lack of inductive bias. To this end, we propose a simple but still effective self-supervised learning (SSL) strategy to train ViTs, that without any external annotation, can significantly improve the results. Specifically, we define a set of SSL tasks based on relations of image patches that the model has to solve before or jointly during the downstream training. Differently from ViT, our RelViT model optimizes all the output tokens of the transformer encoder that are related to the image patches, thus exploiting more training signal at each training step. We investigated our proposed methods on several image benchmarks finding that RelViT improves the SSL state-of-the-art methods by a large margin, especially on small datasets.

1. Introduction

Vision Transformer (ViT) [6] is a model that has been recently developed to address computer vision tasks, such as image classification and object detection. It builds on the Transformer architecture [17], the state of the art in natural language processing, considering patches as parts of the image such as words are parts of a sentence. Although ViT is a valid convolution neural networks (CNNs) competitor, showing comparable and even better results [16], a high-level performance is obtained only when training the model on huge amounts of data. To deal with this issue, aiming at better generalization levels, some recent works modified the attention backbone of ViT introducing hierarchical feature representation [10], progressively tokenization of the image [19] or a shrinking pyramid backbone [18]. Other works, inspired by BERT [4], used self-supervised learning (SSL) paradigm firstly pre-training ViT on a massive amount of unlabelled data and, subsequently, training a linear classifier over the frozen feature of the model or fine-

tuning the pre-trained model to a downstream task [2, 3].

These variants outperform similar-size ResNet both trained on ImageNet, however experiments carried out on smaller datasets are still limited. In this paper, we investigate ViTs on small datasets introducing self-supervised tasks, easily integrated in the original architecture, which face the problem of learning spatial relations among couples of image patches.

In particular: (i) We propose and investigate various self-supervised tasks based on image patches, naturally used by ViTs, showing the improvement optimizing all input tokens, not only the classification one; (ii) We show that our self-supervised tasks are beneficial for the model under two different settings: when the model is pre-trained from scratch on our SSL tasks and subsequently fine-tuned on classification, and when the model is jointly trained from scratch for classification and SSL tasks; (iii) We show that on small datasets, both ViT and its variants jointly trained from scratch on our self-supervised tasks reach better performance with respect to similar state-of-the-art models and overcome the same architectures trained with supervision.

2. Our Method

The ViT model takes an image $\mathbf{x} \in \mathbb{R}^{C \times H \times W}$ as input, divides it into N patches $\mathbf{x}_p \in \mathbb{R}^{N \times (P^2 \cdot C)}$ of C channels and size (P, P) and makes the output prediction as follows:

$$\mathbf{z}_0 = [\mathbf{x}_{\text{class}}, \mathbf{x}_p^1 \mathbf{E}, \dots, \mathbf{x}_p^N \mathbf{E}] + \mathbf{E}_{\text{pos}} \quad (1)$$

$$\mathbf{z}'_\ell = \text{MSA}(\text{LN}(\mathbf{z}_{\ell-1})) + \mathbf{z}_{\ell-1}, \quad \ell = 1 \dots L \quad (2)$$

$$\mathbf{z}_\ell = \text{MSA}(\text{LN}(\mathbf{z}'_\ell)) + \mathbf{z}'_\ell, \quad \ell = 1 \dots L \quad (3)$$

$$\mathbf{y} = \text{LN}(\mathbf{z}_L^0) \quad (4)$$

where \mathbf{z}_ℓ^i is the i -th token of the ℓ -th layer, \mathbf{E} is the projection matrix of the input patches, $\mathbf{E}_{\text{pos}} \in \mathbb{R}^{(N+1) \times D}$ is the learned positional embedding matrix, $\text{MSA}(\cdot)$ is the multi-head self-attention layer [17], and $\text{LN}(\cdot)$ is the layer normalization block [1]. As done in BERT [4], the model uses a randomly initialized classifier token $\mathbf{x}_{\text{class}}$ that, at the end, is taken as the reference for making the prediction \mathbf{y} .

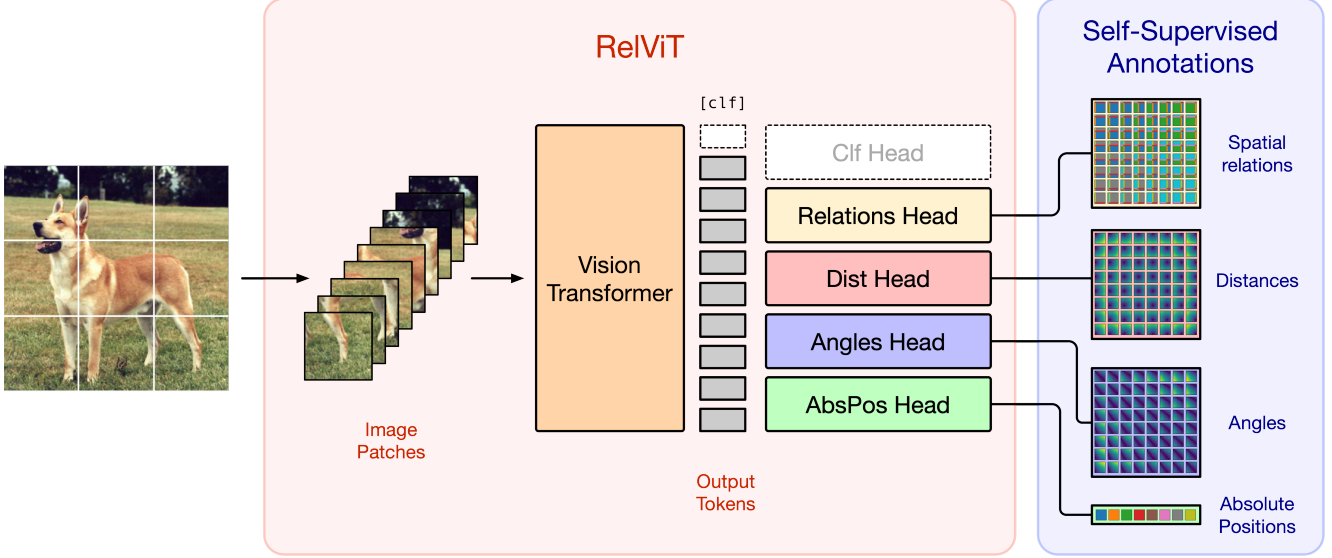


Figure 1. Our RelViT model architecture. The image is partitioned into non-overlapping patches and fed to the vision transformer that produces the output tokens used for the self-supervised tasks.

2.1. Learning From All Tokens

We believe that during the learning process, extending the optimization of the classification token to all the output tokens of ViT could make the model more accurate and the training more efficient. To this end, inspired by [5, 9, 14], we define a list of tasks over the output tokens z_L^i with $i = 1 \dots N$ of the model: *spatial relations* (**SpRel**), to face the problem of recognizing the spatial relation class of couples of image patches, *distances* (**Dist**) and *angles* (**Ang**), to learn a measure of distance and angle, respectively, between the input patches locations in the original image, and, finally, *absolute positions* (**AbsPos**) for recognizing the 2-d location of the input image patch. More formally, referring to z_i with $i = 1 \dots N$ as the i -th token of the L -th layer, given a couple of tokens (z_i, z_j) where z_i is in position $\mathbf{p}_i = (x_i, y_i)$ and z_j is in position $\mathbf{p}_j = (x_j, y_j)$, we let the model to learn the spatial relation r_{ij} defined as:

$$r_{ij} = (s_x, s_y), \quad \text{where} \quad \begin{aligned} s_x &\in \{\text{L, C, R}\} \\ s_y &\in \{\text{T, C, B}\} \end{aligned} \quad (5)$$

where the partial spatial relations $\{\text{L, C, R, T, B}\}$ stand for $\{\text{“left”, “center”, “right”, “top”, “bottom”}\}$. In practice, we let the model to solve the relations classification task over the set of possible spatial relations $r \in \mathcal{R}$ with $|\mathcal{R}| = 9$. We define the distance between the patch locations d_{ij} and the relative angle α_{ij} as:

$$d_{ij} = \|\mathbf{p}_i - \mathbf{p}_j\|. \quad (6)$$

$$\alpha_{ij} = \cos^{-1} \left(\frac{\mathbf{p}_i \cdot \mathbf{p}_j}{\|\mathbf{p}_i\| \|\mathbf{p}_j\| + \epsilon} \right). \quad (7)$$

To avoid numerical problems, in Eq. 7 we add a small positive constant ϵ in the denominator and shift \mathbf{p}_i and \mathbf{p}_j by a constant s . Afterward, we normalize both d_{ij} and α_{ij} in $[-1, 1]$ and train the model to learn the normalized values.

Finally, we define the absolute position of each token z_i simply as i and we let the model solve the classification task over the absolute positions $\{1, \dots, N\}$.

2.2. The Relational Vision Transformer

Our model is depicted in Figure 1. We aim at training all the output tokens processed by the transformer backbone for all the tasks defined in 2.1. Our architecture, dubbed RelViT, uses the standard ViT backbone equipped with specialized heads designed for solving the different tasks which take the output tokens $\mathbf{z} \in \mathbb{R}^{N \times D}$ of the transformer encoder as inputs. Specifically, *Relations*, *Dist* and *Angles* heads, which process couple of tokens, are characterized by a MSA layer that produces the attention scores $\phi(\mathbf{z}, \mathbf{z}) \in \mathbb{R}^{N \times N \times K}$ described as follows:

$$\phi(\mathbf{z}, \mathbf{z}) = [\mathbf{a}_1, \dots, \mathbf{a}_K], \quad \mathbf{a}_i = \frac{\mathbf{z} \mathbf{W}_i \mathbf{z}^T}{\sqrt{D}} \quad (8)$$

where $\mathbf{a}_i \in \mathbb{R}^{N \times N}$ is the attention scores of the single attention head, $\mathbf{W}_i \in \mathbb{R}^{D \times D}$ is a learnable projection matrix, K is the output dimension of the head, and D is the token dimension. Instead, the *AbsPos* head uses a fully connected layer that produces the logits $\phi(\mathbf{z}) \in \mathbb{R}^{N \times K}$ as follows:

$$\phi(\mathbf{z}) = \mathbf{z} \mathbf{W} + \mathbf{b} \quad (9)$$

where $\mathbf{W} \in \mathbb{R}^{D \times K}$ and $\mathbf{b} \in \mathbb{R}^K$ are respectively the weights and bias of the fully connected layer.

Given the corresponding logits, the self-supervised losses are computed as in the following equations:

$$\mathcal{L}_{\text{sp-rel}}(\mathbf{z}) = \frac{1}{N^2} \sum_{i=1}^N \sum_{j=1}^N \text{CE}[\phi_{\text{sp-rel}}(\mathbf{z}_i, \mathbf{z}_j), r_{ij}] \quad (10)$$

$$\mathcal{L}_{\text{dist}}(\mathbf{z}) = \frac{1}{N^2} \sum_{i=1}^N \sum_{j=1}^N \|\phi_{\text{dist}}(\mathbf{z}_i, \mathbf{z}_j) - d_{ij}\|^2 \quad (11)$$

$$\mathcal{L}_{\text{angle}}(\mathbf{z}) = \frac{1}{N^2} \sum_{i=1}^N \sum_{j=1}^N \|\phi_{\text{angle}}(\mathbf{z}_i, \mathbf{z}_j) - \alpha_{ij}\|^2 \quad (12)$$

$$\mathcal{L}_{\text{abs-pos}}(\mathbf{z}) = \frac{1}{N} \sum_{i=1}^N \text{CE}[\phi_{\text{abs-pos}}(\mathbf{z}_i), i] \quad (13)$$

where $\text{CE}(\cdot)$ is the cross-entropy with logits loss function. Finally, during training, we minimize the sum of all the losses of the tasks we want to solve. It is worth noticing that with this formulation, for each training step, we optimize all the combinations of couples of patches at the same time in parallel.

3. Experiments

We aim to demonstrate the effectiveness of learning Visual Transformers via a number of self-supervised tasks whose benefits are shown on both ViT and two of its variants: Swin [10] and T2T-ViT [19].

3.1. Datasets and Implementation Details

Datasets and RelViT Configurations. We conducted experiments on standard image benchmarks for classification focusing on relatively small datasets providing a simple and effective way of boosting ViTs performance. In particular, we tested RelViT on CIFAR-10 [7], SVHN [12], CIFAR-100 [7], Flower-102 [13] and TinyImagenet [8], which have a number of train samples from 1k for Flower-102 to 100k for TinyImagenet. We used ViT-S backbone configuration [2] (model details in Table 1), while the experiments on ViT variants use Swin-T and T2T-ViT-14 backbones with the same model configurations as in [9].

Training Details. We developed our model in PyTorch [15] and the code is publicly available on GitHub¹. For all the experiments, we use the same configurations of the training parameters, except if differently mentioned. All the models are trained for 100 epochs both in the pre-training, fine-tuning and in the downstream-only experiments. Following [2], we use the AdamW [11] optimizer with a cosine learning rate scheduling, linear warm-up of 10 epochs, and $lr = 0.0005$ as the maximum value for the learning rate. We found that RelViT does not need regularization, so we avoid the use of dropout, drop-path, weight

Model	Img Res.	Blocks	Heads	Dim	#Tokens	#Params
ViT-S/4	(32, 32)	12	6	384	65	21.3M
ViT-S/8	(64, 64)	12	6	384	65	21.4M
ViT-S/32	(224, 224)	12	6	384	50	22.5M

Table 1. The used ViTs model configurations. “Img Res.” is the image resolution, “Blocks” and “Heads” are the number of layers in the backbone and of heads in the multi-head self attention layer, “Dim” is the dimension of the token in the transformer encoder, “#Tokens” is the number of patches coming from the image and “#Params” is the number of learnable parameters of the model.

decay, and label smoothing. The batch size is set to 256 for ViT backbone and 64 for its variants, and we use a single GPU for performing each experiment. The data augmentation for the classification problem follows the standard practice of resized crops and random horizontal flipping. Instead, when using ViT backbone and SSL tasks, each image patch is randomly resized-cropped, and following [3] a color shift with color-jittering is applied as well as random gray-scale perturbation.

3.2. Experimental Results

We investigated our RelViT model under two different scenarios: pre-training the model from scratch for our SSL tasks and subsequently fine-tuning on classification (from now on referred as to *pre-training* and *fine-tuning*, respectively) and training the model from scratch jointly on classification and SSL tasks (*downstream-only*). We used the spatial relations and the absolute positions tasks in both pre-training and downstream-only (more details in paragraph 3.3) and we removed the positional encodings in the pre-training, while they are used as aid in the classification task during both fine-tuning and downstream-only.

Table 2 shows RelViT accuracy after a supervised fine-tuning; pre-training and fine-tuning are both obtained on classification, and reported as reference. Our approach leads to higher accuracy than the supervised one in all datasets, gaining +10.01% on Tiny-Imagenet, +6.45% on CIFAR-100 and +4.75% on CIFAR-10. The first row in Table 3 shows RelViT results on classification with downstream-only (using ViT as backbone). Also this configuration improves the results on almost all the datasets up to +4.02% on Flower102, +3.93% on CIFAR-100, and +3.71% on CIFAR-10. The improvements obtained in both scenarios demonstrate the effectiveness of our self-supervised tasks for image classification.

Finally, we investigated how our SSL tasks generalize across different backbones. We chose Swin [10] and T2T-ViT [19] to compare our method with [9] that shares a similar setting. As reported in Table 3, we outperform the supervised baselines and also [9] results up to +19.85% and +16.24% on Flower-102, with Swin and T2T-ViT back-

¹<https://github.com/guglielmocamporese/relvit>

	Backbone	Supervised	RelViT	Improv.
CIFAR-10	ViT-S/4	85.38	90.13	+4.75 ↑
SVHN	ViT-S/4	96.07	97.15	+1.08 ↑
CIFAR-100	ViT-S/4	58.01	64.46	+6.45 ↑
Flower-102	ViT-S/32	41.67	45.49	+3.82 ↑
TinyImagenet	ViT-S/8	42.09	52.10	+10.01 ↑

Table 2. Comparison between our RelViT model and the supervised ViT baselines on several small datasets. RelViT is pre-trained on our SSL tasks and subsequently finetuned for classification, whereas the baselines are trained on classification.

Backbone	Method	CIFAR-10	SVHN	CIFAR-100	Flower-102
ViT [6]	Supervised	ViT-S/4	ViT-S/4	ViT-S/4	ViT-S/32
		85.18	96.02	58.11	40.59
	RelViT (our)	88.98	95.86	62.04	44.61
	(Improv.)	(+3.8 ↑)	(-0.16 ↓)	(+3.93 ↑)	(+4.02 ↑)
Swin [10]	Supervised [9]	59.47	71.6	53.28	34.51
	Swin+ \mathcal{L}_{drloc} [9]	83.89	94.23	66.23	39.37
	RelSwin (our)	92.17	96.55	69.97	59.22
	(Improv.)	(+8.28 ↑)	(+2.32 ↑)	(+3.74 ↑)	(+19.85 ↑)
T2T-ViT [19]	Supervised [9]	84.19	95.36	65.16	31.73
	T2T-ViT+ \mathcal{L}_{drloc} [9]	87.56	96.49	68.03	34.35
	RelT2T-ViT (our)	91.08	96.52	66.27	50.59
	(Improv.)	(+3.52 ↑)	(+0.03 ↑)	(-1.76 ↓)	(+16.24 ↑)

Table 3. Comparison of our method with other works on multiple backbones. The results are obtained training the model from scratch jointly on our self-supervised tasks and classification.

bones, respectively.

3.3. Ablations

SSL Multi-Task Ablation. We defined multiple SSL tasks over the image tokens and evaluated each combination of tasks in order to highlight both the importance of each sub-problem and the relations among them. As shown in Table 4, that displays our results, solving, individually, each SSL task leads to similar fine-tuning accuracy, improving the performance w.r.t the supervised baseline of +3.00% on average. Among SSL tasks, the *SpRel* one is the most performing and the optimal combination of tasks is obtained by learning the *SpRel* and the *AbsPos* of the patches.

Positional Embeddings and Patches Permutations. We investigated the shortcut learning problem in RelViT using the positional embeddings (PEs) during the self-supervised pre-training. Moreover, to avoid trivial solutions and break the dependency between PEs and SSL labels, we investigated the shuffling of the input patches before adding the PEs, permuting the rows and columns of the label matrix with the same permutation used for shuffling the input tokens. Since we aim at focusing on the role of the PEs and the patch shuffling, for simplicity we used only the *SpRel* learning on the pre-training. As shown in Figure 2a, if the model uses the PEs without shuffling during the pre-training, it solves the task with 100% of *SpRel* accuracy but

Method	AbsPos (Acc ↑)	Ang (MSE ↓)	Dist (MSE ↓)	SpRel (Acc ↑)	Finetuning (Acc ↑)
Supervised	×	×	×	×	85.38
RelViT	×	×	×	48.53	89.02
RelViT	×	×	10.54	×	89.27
RelViT	×	13.08	×	×	88.75
RelViT	15.24	×	×	×	89.39
RelViT	×	×	10.29	48.91	89.24
RelViT	×	12.55	×	48.66	90.12
RelViT	15.73	×	×	48.53	90.13
RelViT	×	12.58	10.32	×	89.34
RelViT	16.03	×	10.49	×	89.75
RelViT	15.51	12.82	×	×	89.90
RelViT	×	12.49	10.28	48.98	88.81
RelViT	15.90	×	10.39	48.67	89.80
RelViT	16.03	12.52	×	48.80	89.73
RelViT	16.06	12.65	10.50	×	89.67
RelViT	16.07	12.54	10.39	48.74	90.06

Table 4. Results using our SSL tasks on CIFAR-10 with ViT-S/4 backbone. The columns from the 2nd to the 6th report the performance on the SSL tasks whereas the last column is the accuracy of the fine-tuned models.

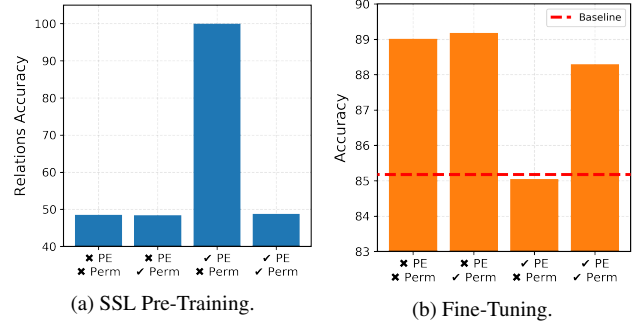


Figure 2. The role of the positional embedding (PE) and random permutations (Perm) of the input patches in RelViT.

the corresponding fine-tuned model reaches a classification accuracy comparable to a randomly initialized network (red dashed line in Fig. 2b). Even though the shuffling removes the trivial solution and improves the classification accuracy, we removed PEs from RelViT since, in this way, we obtained the best results. Whereupon, the shuffling is optional due to the permutation equivariance property of the model.

4. Conclusion

In this work, we have proposed and investigated several SSL tasks defined over image patches to improve ViT ability on small datasets. Our proposed methods are straightforward to implement and effective as RelViT shows significant improvement on all the tested datasets and in both scenarios: pre-training on SSL tasks and then fine-tuning and training jointly on SSL and SL tasks.

References

- [1] Jimmy Ba, Jamie Ryan Kiros, and Geoffrey E. Hinton. Layer normalization. *ArXiv*, abs/1607.06450, 2016. 1
- [2] Mathilde Caron, Hugo Touvron, Ishan Misra, Herve Jegou, Julien Mairal, Piotr Bojanowski, and Armand Joulin. Emerging properties in self-supervised vision transformers. In *ICCV*, 2021. 1, 3
- [3] Xinlei Chen and Kaiming He. Exploring simple siamese representation learning. In *CVPR*, 2021. 1, 3
- [4] Jacob Devlin, Ming-Wei Chang, Kenton Lee, and Kristina Toutanova. Bert: Pre-training of deep bidirectional transformers for language understanding. In *NAACL*, 2019. 1
- [5] Carl Doersch, Abhinav Gupta, and Alexei A. Efros. Unsupervised visual representation learning by context prediction. In *ICCV*, 2015. 2
- [6] Alexey Dosovitskiy, Lucas Beyer, Alexander Kolesnikov, Dirk Weissenborn, Xiaohua Zhai, Thomas Unterthiner, Mostafa Dehghani, Matthias Minderer, Georg Heigold, Sylvain Gelly, Jakob Uszkoreit, and Neil Houlsby. An image is worth 16x16 words: Transformers for image recognition at scale. *ICLR*, 2021. 1, 4
- [7] Alex Krizhevsky. Learning multiple layers of features from tiny images. 2009. 3
- [8] Ya Le and Xuan Yang. Tiny imagenet visual recognition challenge. 2015. 3
- [9] Yahui Liu, Enver Sangineto, Wei Bi, Nicu Sebe, Bruno Lepri, and Marco De Nadai. Efficient training of visual transformers with small-size datasets. *NeurIPS*, 2021. 2, 3, 4
- [10] Ze Liu, Yutong Lin, Yue Cao, Han Hu, Yixuan Wei, Zheng Zhang, Stephen Lin, and Baining Guo. Swin transformer: Hierarchical vision transformer using shifted windows. In *ICCV*, 2021. 1, 3, 4
- [11] Ilya Loshchilov and Frank Hutter. Decoupled weight decay regularization. In *ICLR*, 2019. 3
- [12] Yuval Netzer, Tao Wang, Adam Coates, Alessandro Bis-sacco, Bo Wu, and Andrew Y. Ng. Reading digits in natural images with unsupervised feature learning. In *NIPS Workshop on Deep Learning and Unsupervised Feature Learning*, 2011. 3
- [13] Maria-Elena Nilsback and Andrew Zisserman. Automated flower classification over a large number of classes. *Proc. of Indian Conference on Computer Vision, Graphics & Image Processing*, 2008. 3
- [14] Mehdi Noroozi and Paolo Favaro. Unsupervised learning of visual representations by solving jigsaw puzzles. In *ECCV*, 2016. 2
- [15] Adam Paszke, Sam Gross, Francisco Massa, Adam Lerer, James Bradbury, Gregory Chanan, Trevor Killeen, Zeming Lin, Natalia Gimelshein, Luca Antiga, Alban Desmaison, Andreas Kopf, Edward Yang, Zachary DeVito, Martin Raison, Alykhan Tejani, Sasank Chilamkurthy, Benoit Steiner, Lu Fang, Junjie Bai, and Soumith Chintala. Pytorch: An imperative style, high-performance deep learning library. In *NeurIPS*, 2019. 3
- [16] Maithra Raghu, Thomas Unterthiner, Simon Kornblith, Chiyuan Zhang, and Alexey Dosovitskiy. Do vision transformers see like convolutional neural networks? In *arXiv:2108.08810*, 2021. 1
- [17] Ashish Vaswani, Noam Shazeer, Niki Parmar, Jakob Uszkoreit, Llion Jones, Aidan N Gomez, Łukasz Kaiser, and Illia Polosukhin. Attention is all you need. In *NeurIPS*, 2017. 1
- [18] Wenhai Wang, Enze Xie, Xiang Li, Deng-Ping Fan, Kaitao Song, Ding Liang, Tong Lu, Ping Luo, and Ling Shao. Pyramid vision transformer: A versatile backbone for dense prediction without convolutions. In *ICCV*, 2021. 1
- [19] Li Yuan, Yunpeng Chen, Tao Wang, Weihao Yu, Yujun Shi, Zi-Hang Jiang, Francis EH Tay, Jiashi Feng, and Shuicheng Yan. Tokens-to-token vit: Training vision transformers from scratch on imagenet. In *ICCV*, 2021. 1, 3, 4